Supporting Information

# Shape-Control of $CeF_3$ Nanocrystals by Doping Polyoxometalates: Syntheses, Characterization and Tunable Photoluminescence

Guan Wang,[a] Ruru Meng,[a] Jing Yang,[a] Xiaomei He,[a] Jingjing Chen,[a] Dongdi Zhang[a], Xiangxing Xu*[b] and Jingyang Niu*[a]

*a. Henan Key Laboratory of Polyoxometalate Chemistry, Institute of Molecular and Crystal Engineering, College of Chemistry and Chemical Engineering, Henan University, Kaifeng, Henan, China. E-mail: jyniu@henu.edu.cn*

*b. School of Chemistry and Materials Science, Nanjing Normal University, Nanjing 210023, PR China. E-mail: xuxx@njnu.edu.cn*

## Experimental section

### Materials and methods

$Ce(NO_3)_3{\cdot}6H_2O$ (99%), polyvinylpyrrolidone (PVP), and $KBF_4$ (99%) were purchased without further purification. α-$PMo_{12}$, α-$PW_{12}$, and α-$SiW_{12}$ were synthesized according to ref [1]. The scanning electron microscopy (SEM) images and EDX spectra were obtained on a JSM−7610F scanning electron microscopy with an acceleration voltage of 10 kV. To characterize the nanocrystals phase, X−ray diffractions (XRD) were performed on a Bruker D8 Advance instrument with Cu Ka radiation ($\lambda$ = 1.5418 Å). IR spectra were recorded on an avatar 360 fourier transform infrared spectrophotometer using KBr pellets in the range of 4000−500 $cm^{-1}$. The X-ray photoelectron spectra (XPS) were collected using Thermo ESCALAB 250XI. TG analysis was conducted with a Mettler-Toledo TGA/SDTA851 instrument. The PL spectra were collected by a Hitachi F–7000 fluorescence spectrophotometer. The PL lifetime was performed on an Edinburgh Instruments FLS980 spectrophotometer.

### Preparation of $PMo_{12}/CeF_3$ nanoflower

In a typical procedure, $Ce(NO_3)_3{\cdot}6H_2O$ (0.130 g, 0.299 mmol), PVP (0.050 g), $KBF_4$ (0.151g, 1.199 mmoL) and α-$PMo_{12}$ (0.050 g, 0.026 mmoL) were added into 18.5 mL aqueous solution. After vigorous stirring for 30 min, the mixture was transferred to a Teflon-lined autoclave (25 mL) and kept at 140 °C for 10 h. After slow cooling to room temperature naturally, the yellow precipitates of $PMo_{12}/CeF_3$ NCs were separated by centrifugation, and washing with deionized water and ethanol to remove excess reagents.

### Preparation of $SiW_{12}/CeF_3$ nanoplate

The synthetic procedure was identical to flower-like $PMo_{12}/CeF_3$ NCs, but α-$SiW_{12}$ (0.015 g, 0.005 mmoL) was used as dopants to replace α-$PMo_{12}$. After hydrothermal procedure, white solid product was obtained, washing with deionized water and ethanol for purification.

### Preparation of $PW_{12}/CeF_3$ nanosphere

$PW_{12}/CeF_3$ nanospheres were also prepared according to the method of flower-like $PMo_{12}/CeF_3$ NCs, but α-$PW_{12}$ (0.040 g, 0.014 mmoL) was used instead of α-$PMo_{12}$. White product was collected after the experiment. The resulting $PW_{12}/CeF_3$ NCs were purified by washing with deionized water and ethanol to removed excess amorphous powder and organic ligands.

### Synthetic and discussion

### Control experiments

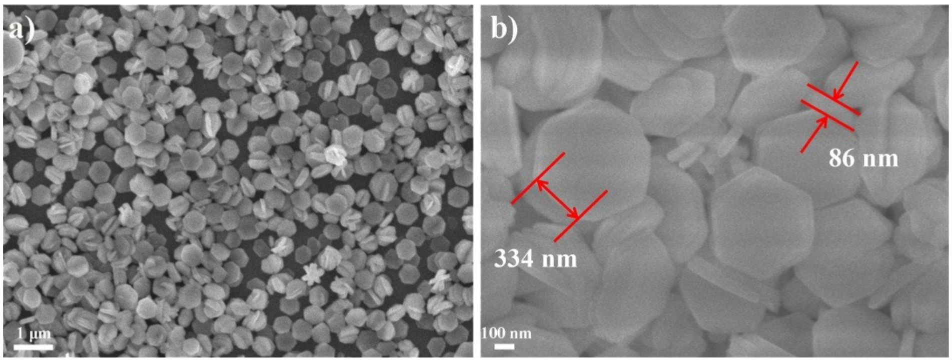

Fig. S1 SEM images of $CeF_3$ NCs with hexagonal shape.

| amount of dopants | $PMo_{12}/CeF_3$ | $SiW_{12}/CeF_3$ | $PW_{12}/CeF_3$ |
|---|---|---|---|
| 0.005 mmol | Plate | Plate | Plate |
| 0.008 mmol | Plate | Sphere | Plate |
| 0.014 mmol | Plate and Flower | Sphere | Sphere |
| 0.026 mmol | Flower | Flower | Amorphous |
| 0.053 mmol | Amorphous | Amorphous | Amorphous |

Table S1 Shape List of $POM/CeF_3$ in control experiments.

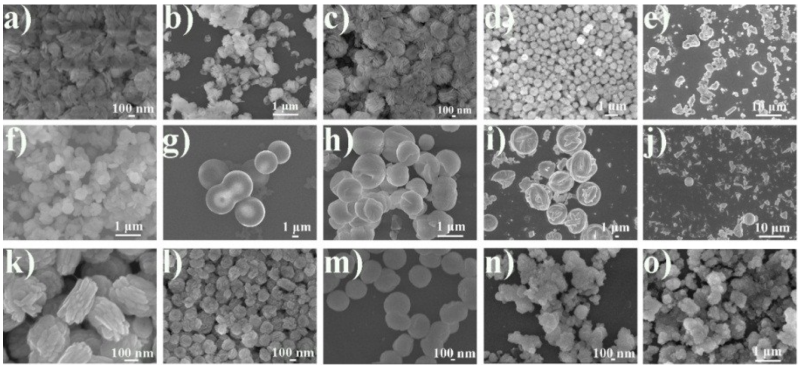

Fig. S2 SEM images of POM/$CeF_3$ NCs with different amount of dopants.

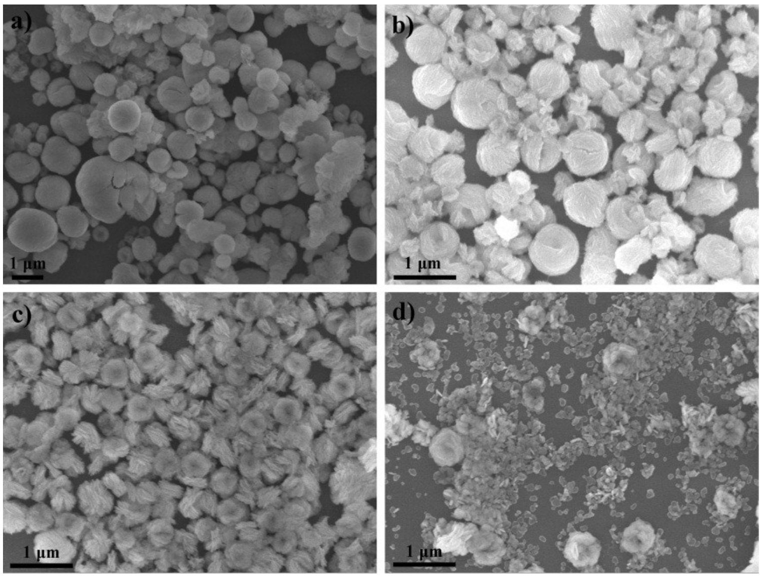

Fig. S3 SEM images of $PMo_{12}/CeF_3$ obtained with increasing reaction temperatures: (a) 40 °C, (b) 80 °C, (c) 120 °C, and (d) 180 °C.

Taking $PMo_{12}/CeF_3$ as an example, control experiments were carried out to explore the reaction system of POM/$CeF_3$. Considering the nanoflower could be affected by reaction temperature, another set of control experiments were investigated under different temperatures. When the experiment was carried out around 40 ºC, a few flower-like particles were obtained. As shown in Fig. S3, amorphous bulks are observed, and the rest of particles represent irregular shape. With the rising of temperature, nanoflowers with a broad size distribution were gradually increased (Fig. S3b). When further raising the temperature to 120 ºC, the shape of $PMo_{12}/CeF_3$ NCs became uniform. However, most of the flowers show incomplete structures (Fig. S3c). When the temperature exceeding 180 ºC, lots of fragmentized NCs are collected (Fig. S3d), indicating high temperature would destroy the uniform structure.

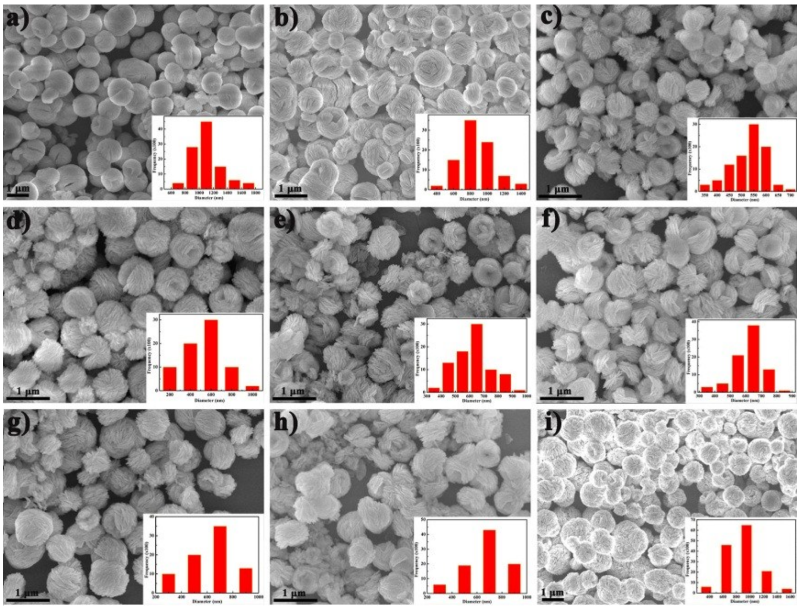

Fig. S4 SEM images of $PMo_{12}/CeF_3$ prepared under different reaction times: (a) 0.5 hr, (b) 1 hr, (c) 2 hrs, (d) 4 hrs, (e) 6 hrs, (f) 8 hrs, (g) 12 hrs, (h) 14 hrs and (i) 24 hrs, inset: size distribution of the $PMo_{12}/CeF_3$ nanoflower.

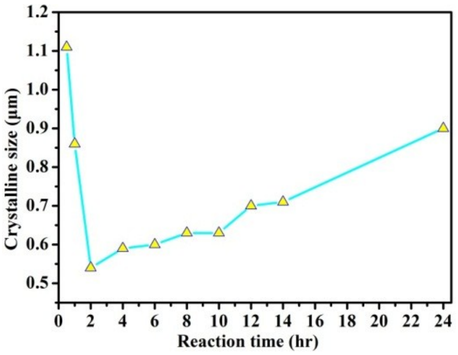

Fig. S5 Plot of the crystalline size when the reaction time was increasing.

Reaction time is another important factor in the synthetic process. As shown in Fig. S4, ten different times were employed to study the influence on nanoflower shape. When the reaction time was less than 1 hr, $PMo_{12}/CeF_3$ particles were formed (Fig. S4a, S4b). These particles show nearly no flower-like shape, but it can be observed clearly that the particle is constructed by nanosheets. From Fig. S4c to S4i, the SEM images present the shape of $PMo_{12}/CeF_3$ NCs under the reaction time between 2 hrs and 24 hrs. It is seen that the $PMo_{12}/CeF_3$ particles has changed to flower-like shape with the increasing of reaction time. The crystalline size of $PMo_{12}/CeF_3$ depends on reaction time which is clearly shown in Fig. S5.

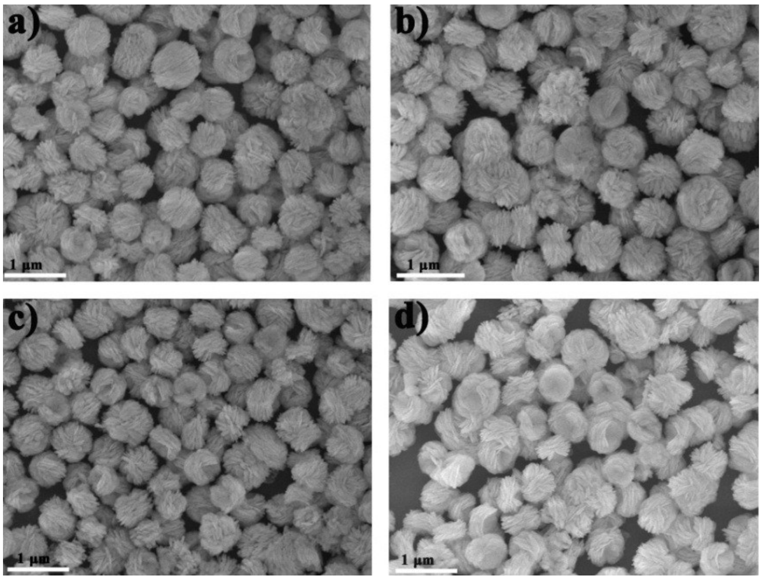

Fig. S6 Stability research of $PMo_{12}/CeF_3$ nanoflower in aqueous solution. (Immersing time, a: 12 hrs, b: 24 hrs, c: 36 hrs, d: 48 hrs).

As shown in Fig. S6, this kind of $PMo_{12}/CeF_3$ nanoflower reveals strong stability in water solution over time. The uniform shape remains unchanged in 48 hrs. Thus, the stability endow $PMo_{12}/CeF_3$ nanoflower has the actual application value in solution system.

## Characterization

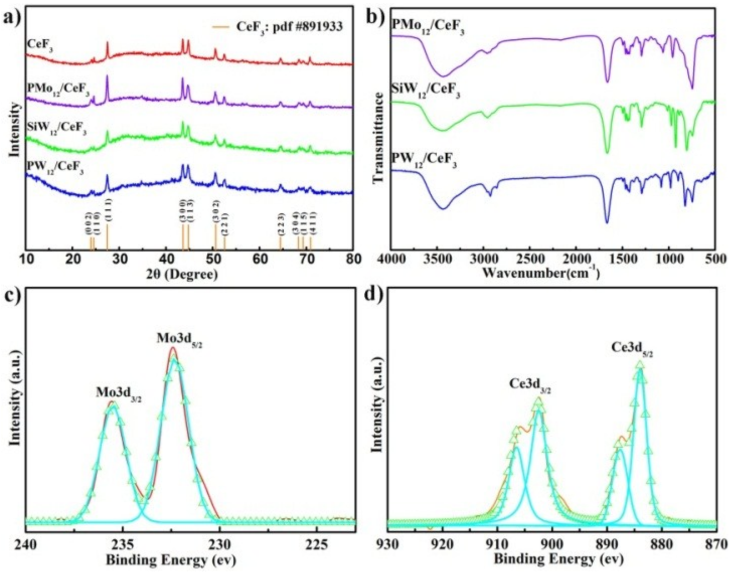

Fig. S7 (a) XRD pattern of $CeF_3$, $PMo_{12}/CeF_3$, $SiW_{12}/CeF_3$ and $PW_{12}/CeF_3$; (b) IR spectra of $PMo_{12}/CeF_3$, $SiW_{12}/CeF_3$ and $PW_{12}/CeF_3$; XPS spectra of $PMo_{12}/CeF_3$: (c) $Mo3d_{3/2}$ and $Mo3d_{5/2}$; (d) $Ce3d_{3/2}$ and $Ce3d_{5/2}$ (orange/red line: experimental data; green scatter: fitting curve; cyan line: spin–orbit partner lines)

Fig. S7a shows the XRD patterns of as-prepared $CeF_3$, $PMo_{12}/CeF_3$, $SiW_{12}/CeF_3$ and $PW_{12}/CeF_3$. These XRD patterns are consistent with the primitive hexagonal structured $CeF_3$ (pdf no. 891933), indicating these samples are well crystallized. The 2θ peaks at around 27.5°, 43.9°, 44.8°, 50.5°, 52.5° are corresponding to the (111), (300), (113), (302) and (221) crystal planes, respectively. It should be pointed out that the signal of POMs cannot be detected in this test. The possible reason is that the content of POMs is lower than $CeF_3$ in each sample. Therefore, the diffraction peaks of POMs are relatively weak, so that the peaks could be overlapped and covered. POMs have characteristic vibration peaks which could be certified by means of IR spectra. As depicted in Fig. S7b, the characteristic bands appearing at 1061 $cm^{-1}$ (P–O), 957 $cm^{-1}$ (Mo–O) and 876 $cm^{-1}$ (Mo–O–Mo) in the spectrum of $PMo_{12}/CeF_3$, demonstrating the existence of α-$PMo_{12}$ [2]. In addition, in the spectrum of $SiW_{12}/CeF_3$, vibration bands at 972, 924 and 885 $cm^{-1}$ are assigned to $\nu(W–O_d)$, $\nu(Si–O_a)$ and $\nu(W–O_b–W)$, respectively [3]. This result also proves the successful doping of α-$SiW_{12}$. Finally, a typical spectrum of α-$PW_{12}$ is determined in $PW_{12}/CeF_3$, the peaks at 1081, 980 and 897 $cm^{-1}$ is attributed to the O–P–O, $W–O_d$ and $W–O_b–W$ bands, respectively [4]. As a consequence, the combination of XRD patterns and IR spectra can clearly reveal the components of POM/$CeF_3$ compounds. The XPS investigations on $PMo_{12}/CeF_3$ nanoflower were performed to confirm the valence states of Ce and Mo. The XPS spectra of Mo centers: the peaks around 235.6 and 232.5 eV in the energy regions of $Mo3d_{3/2}$ and $Mo3d_{5/2}$ are confirmed to be $Mo^{6+}$ centers represented in Fig. S7c [5]. The XPS spectra of Ce centers (Fig. S7d): the peaks around 902.4 and 884.0 eV in the energy regions of $Ce3d_{3/2}$ and $Ce3d_{5/2}$ correspond to $Ce^{3+}$ ions [6].

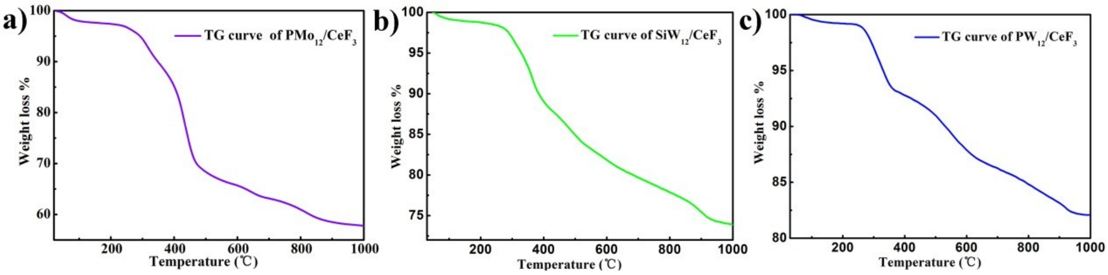

Fig. S8 TG curves of $PMo_{12}/CeF_3$, $SiW_{12}/CeF_3$ and $PW_{12}/CeF_3$.

Thermogravimetric (TG) experiments have been conducted to study the thermal stability of $PMo_{12}/CeF_3$, $SiW_{12}/CeF_3$ and $PW_{12}/CeF_3$, which are important parameters of these nanomaterials. The TG curves are shown in Fig. S8, which have been analyzed in air dynamic atmosphere at a heating rate of 10 ºC/min in the range of 25–1000 ºC and 10.027, 11.849 and 10.436 mg samples are used in the form of powder, respectively. As depicted in Fig. S8a, The weight loss of $PMo_{12}/CeF_3$ can be divided into three steps. The weight loss of 2.2% during the first step from 25 to 120 ºC involves the loss of adsorbed water molecules. On further heating, the material lose weight continuously during the second step with the weight loss of 28.97% from 120 to 490 ºC, corresponding to the removal of PVP molecules. The third weight loss of 11.05% occurs between 490 and 1000 ºC, resulting from the oxidation of $CeF_3$. As shown in Fig. S8b, the TG curve of $SiW_{12}/CeF_3$ gives a total weight loss of 26.13% in the range of 25–1000 ºC. The weight loss of 1.58% during the first step from 25 to 250 ºC corresponds to the release of adsorbed water molecules. The second weight loss of 14.33% between 250–520 ºC is approximately attributed to the removal of PVP molecules. The third weight loss of 10.22% from 520 to 1000 ºC results from the oxidation of $CeF_3$. For $PW_{12}/CeF_3$, the total loss is 17.92% in the range of 25–1000 ºC (Fig. S8c). The first weight loss is 0.86% from 25 to 235 ºC, assigned to the release of adsorbed water, and followed by the loss of 5.95% approximating the removal of PVP molecules from 235 to 370 ºC. The third weight loss of 11.11% from 370 to 1000 ºC is observed and assigned to the oxidation of $CeF_3$.

| Sample | Emission (nm) | $\tau_1$ (ns) | $\tau_2$ (ns) | $a_1$ | $a_2$ | R-Square | $\tau_{av}$ (ns) |
|---|---|---|---|---|---|---|---|
| $CeF_3$ | 324 | 19.06 | | 1.01 | | 0.994 | 19.06 |
| $PMo_{12}/CeF_3$ | 305 | 1.00 | 7.19 | 1.37 | 0.29 | 0.997 | 4.72 |
| $SiW_{12}/CeF_3$ | 333 | 6.26 | 20.61 | 0.49 | 0.51 | 0.999 | 17.34 |
| $PW_{12}/CeF_3$ | 332 | 4.82 | 16.99 | 0.74 | 0.34 | 0.999 | 12.35 |

Table S2 Fitting parameters of the PL decay curves.

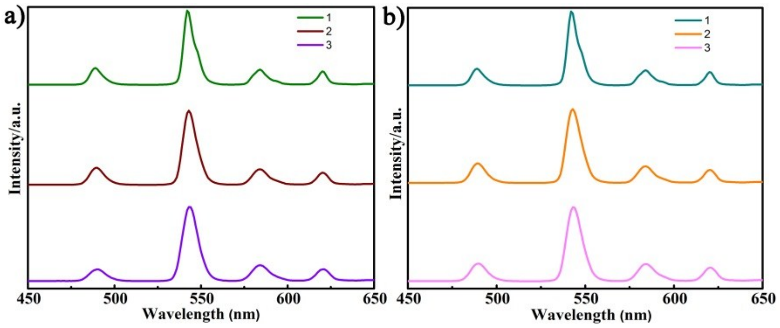

Fig. S9 (a) Emission spectra of $CeF_3:Tb^{3+}$ (line **1**), $PMo_{12}/CeF_3:Tb^{3+}$ (dopant: 0.10 mmol α-$PMo_{12}$, line **2**) and $PMo_{12}/CeF_3:Tb^{3+}$ (dopant: 0.20 mmol α-$PMo_{12}$, line **3**); (b) Emission spectra of $CeF_3:Tb^{3+}$ (line **1**), $PMo_{12}/CeF_3:Tb^{3+}$ (dopant: 0.30 mmol α-$PMo_{12}$, line **2**) and $PW_{12}/CeF_3:Tb^{3+}$ (dopant: 0.30 mmol α-$PW_{12}$, line **3**).

Rare earth (RE) ions are always used as dopants to enhance the PL of $CeF_3$ [7-8]. In order to determine whether the emission of RE ions could also be controlled by doping POMs, additional tests have been carried out. According to the methods of preparing $CeF_3$ NCs, $PMo_{12}/CeF_3$ NCs and $PW_{12}/CeF_3$ NCs, $Tb(NO_3)_3 \cdot 6H_2O$ (0.015 g, 0.033 mmol, 99.99%, purchased from Acros without further purification) has been introduced into these reaction systems. The emission spectra of $CeF_3$ NCs and different doping amount of $PMo_{12}/CeF_3$ are shown in Fig. S9a. Under excitation at 250 nm, these samples display typical emission peaks of $Tb^{3+}$ ions, at 489 nm, 542 nm, 584 nm and 620 nm. These results indicate that the doping of α-$PMo_{12}$ could not change the emission of $Tb^{3+}$ ions, even if the doping amounts are changed. As depicted in Fig. S9b, the emission spectra of $CeF_3:Tb^{3+}$, $PMo_{12}/CeF_3:Tb^{3+}$ and $PW_{12}/CeF_3:Tb^{3+}$ are obtained under excitation at 250 nm. Equivalent amounts of α-$PMo_{12}$ and α-$PW_{12}$ are used as dopants to investigate the emission spectra. Compared to the emission peaks of $Tb^{3+}$ ions, the doping of α-$PMo_{12}$ and α-$PW_{12}$ could also not change the PL property of RE ions.

To sum up, these phenomena illustrate that the emission of $CeF_3$ could be tuned by doping POMs. However, this method may not an effective way to control the PL of RE ions. In the upcoming research, we will continue to systematic probe and explore the interaction between different POMs and RE ions.

## Notes and references

[1] C. R. Deltcheff, M. Fournier, R. Franck and R. Thouvenot, Inorg. Chem., 1983, 22, 207–216.

[2] H. Kim, J. C. Jung, P. Kim, S. H. Yeom, K. Y. Lee and I. K. Song, J. Mol. Catal. A. Chem., 2006, 259, 150–155.

[3] C. R. Deltcheff, M. Fournier, R. Franck and R. Thouvenot, Inorg. Chem., 1983, 22, 207–216.

[4] G. G. Papagianni, D. V. Stergiou, G. S. Armatas, M. G. Kanatzidis and M. I. Prodromidis, Sensor. Actuat. B. Chem., 2012, 173, 346–353.

[5] J. H. Yang, F. Y. Lu, Y. Li, S. X. Yang, R. X. Li, N. J. Huo, C. Fan, Z. M. Wei, J. B. Li and S. S. Li, J. Mater. Chem. C., 2014, 2, 1034–1040.

[6] W. C. Chen, C. Qin, X. L. Wang, Y. G. Li, H. Y. Zang, K. Z. Shao, Z. M. Su and E. B. Wang, Dalton. Trans., 2015, 44, 11290–11293.

[7] S. Gai, P. Yang, X. Li, C. Li, D. Wang, Y. Dai and J. Lin, J. Mater. Chem., 2011, 21, 14610–14615.

[8] T. Samanta, S. Sarkar, V. N. K. B. Adusumalli, A. Praveen and V. Mahalingam, Dalton Trans., 2016, 45, 78–84.